ELSEVIER

European Journal of Pharmacology 404 (2000) 79–88

ejp

www.elsevier.nl/locate/ejphar

Rabies virus infection prevents the modulation by α_2-adrenoceptors, but not muscarinic receptors, of Ca^{2+} channels in NG108-15 cells

Masashi Iwata [a], Toshihio Unno [a], Nobuyuki Minamoto [b], Hidenori Ohashi [a], Seiichi Komori [a,*]

[a] *Laboratory of Pharmacology, Department of Veterinary Science, Faculty of Agriculture, Gifu University, 1-1 Yanagido, Gifu 501-1193, Japan*
[b] *Laboratory of Veterinary Public Health, Department of Veterinary Science, Faculty of Agriculture, Gifu University, Gifu 501-1193, Japan*

Received 16 March 2000; received in revised form 7 August 2000; accepted 11 August 2000

Abstract

In mouse neuroblastoma × rat glioma hybrid (NG108-15) cells, we examined whether rabies virus infection affects the voltage-dependent Ca^{2+} current (I_{Ca}) and agonist-induced I_{Ca} inhibition. The viral infection had little effect on the current–voltage relationship for peak I_{Ca} or on the late I_{Ca} that remained at the end of a 200-ms step depolarization. Noradrenaline and carbachol, via α_2-adrenoceptors and muscarinic receptors, respectively, reduced I_{Ca} concentration dependently. The maximum effect of noradrenaline was attained at 10 μM with $19.4 \pm 1.8\%$ inhibition of I_{Ca}, which was significantly decreased to $9.9 \pm 1.3\%$ after viral infection. The decrease was not reversed with 100 μM noradrenaline, suggesting that it does not result from a decrease in agonist sensitivity of cells. The maximum effect of carbachol (300 μM; $27.7 \pm 2.9\%$ inhibition) remained unchanged, despite carbachol sharing intracellular signaling pathways with noradrenaline. These results indicate that in NG108-15 cells, rabies virus infection does not alter the functional expression of voltage-dependent Ca^{2+} channels, but it attenuates the α_2-adrenoceptor-mediated I_{Ca} inhibition, possibly through some change at the receptor level.

Keywords: Rabies virus; NG108-15 cell; Ca^{2+} current; α-Adrenoceptor; Muscarinic receptor; Patch clamp, Whole-cell

1. Introduction

Rabies virus infection induces the furious or paralytic form of fetal nervous disorders in humans and a variety of animals including dogs, cats, skunks, horses and bats. The brain and spinal cord are shown to be predilection sites for the viral infection. However, no or only minor histopathological changes are observed in the central nervous system of infected humans and animals (Tirawatnpong et al., 1989; Johnson, 1965). Therefore, it is believed that the pathogenesis of rabies disease is due to functional impairment of virus-infected neurons (Murphy, 1977).

Radioligand binding studies have suggested that rabies virus infection reduces the distribution density and/or agonist-binding affinity of plasma membrane receptors specific for neurotransmitters such as acetylcholine, serotonin, and opiates (Tsiang, 1982; Dumrongphol et al., 1996; Ceccaldi et al., 1993; Munzel and Koschel, 1981). There is a biochemical study suggesting that the viral infection may disrupt coupling of opiate receptors to GTP-binding proteins (G proteins) responsible for the inhibitory regulation of adenylate cyclase (Koschel and Munzel, 1984).

Our recent study of the effects of rabies virus infection on membrane currents of mouse neuroblastoma cells showed that the functional expression of voltage-dependent Na^+ channels and inward rectifier K^+ channels, but not delayed rectifier K^+ channels, is reduced after viral infection (Iwata et al., 1999). Such Na^+ and K^+ channels sensitive to the virus are known to function in neurons as a generator of the upstroke of action potentials and as a determinant of the resting membrane potential, respectively. Neurons also express voltage-dependent Ca^{2+} channels which serve as a major pathway for Ca^{2+} entry, when they are excited, to trigger the release of transmitters. The present study was designed to see whether functional expression of this type of Ca^{2+} channel is modified by viral infection. The effect of rabies virus infection on membrane current flowing through the Ca^{2+} channels (I_{Ca}) was investigated in mouse neuroblastoma × rat glioma hybrid (NG108-15) cells, which are known to

* Corresponding author. Tel.: +81-058-293-2941; fax: +81-058-293-2942.
E-mail address: skomori@cc.gifu-u.ac.jp (S. Komori).

0014-2999/00/$ - see front matter
PII: S0014-2999(00)00621-X

express voltage-dependent Ca^{2+} channels (Tsunoo et al., 1986) and to be sensitive to rabies virus (Munzel and Koschel, 1981). NG108-15 cells express α_2-adrenoceptors and muscarinic receptors, activation of which causes a reduction of I_{Ca} via pertussis toxin-sensitive G proteins (Docherty and McFadzean, 1989; Caulfield and Brown, 1991). This led us also to examine whether viral infection affects receptor-coupled signal transduction, thus causing I_{Ca} inhibition.

2. Materials and methods

2.1. Cell culture

NG108-15 cells used for the present study were obtained from the Laboratory of Veterinary Public Health, Gifu University. They were grown in Dulbecco's modified Eagle's minimum essential medium (from Nissui, Toshima-ku, Tokyo, Japan) in an atmosphere of 5% CO_2. The growth medium contained fetal calf serum (10%), penicillin (10 units/ml), streptomycin (0.01 g/ml), fungizone (2.5 μg/ml), hypoxanthine (100 μM), aminopterin (1 μM), thymidine (16 μM) and $NaHCO_3$ (0.1–0.15%). To accelerate their differentiation before use in the experiments, the cells were cultured in a medium for 10–20 days with medium renewal every 2 or 3 days. The culture medium contained reduced fetal calf serum (1%) and 1 mM dibutyryl cyclic AMP, but the other constituents were the same as those of the growth medium.

2.2. Virus infection

Differentiated cells were removed from the bottom of flasks by gentle shaking and then dispersed by drawing in and out of a grass pipette. The cell suspension was centrifuged at 1500 rpm for 5 min. The sedimented cells were resuspended in fresh culture medium to give 2×10^4 cells/ml and divided into two groups, one of which was inoculated with rabies virus (RC-HL strain, Ito et al., 1994) at an infection multiplicity of 50 plaque forming units per cell, and the other was mock inoculated as control. Each of these cell suspensions was then seeded into a 24-well plate containing poly-L-ornithine-coated glass coverslips (14 mm in diameter) in aliquots of 0.5 ml per well, and placed in a humidified atmosphere of 5% CO_2 at 37°C for 2 days.

An indirect immunofluorescence technique was used to detect intracytoplasmic rabies virus nucleoprotein (N protein), as previously described (Minamoto et al., 1994; Iwata et al., 1999). Briefly, the cells incubated with or without virus inoculum for 2 days were air-dried, and fixed with cold acetone (−20°C) for 15 min. They were then subjected to sequential immunostaining with a mouse monoclonal anti-N protein (Laboratory of Veterinary Public Health, Gifu University) followed by a fluorescein isothiocyanate-conjugated anti-mouse immunoglobulin G rabbit antibody (ICN Immuno Biologicals, CA, USA).

All virus-inoculated cells expressed viral N protein immunoreactivity, indicating their infection with the virus, whereas mock-inoculated cells expressed no such immunoreactivity. The two groups of cells prepared were used as virus-infected and uninfected cells for the following experiments.

2.3. Ca2 + current recordings

A coverslip with virus-infected or uninfected cells was placed in a 0.5-ml organ bath on the stage of an inverted microscope (TMD, Nikon, Chiyoda-ku, Tokyo), and the organ bath was washed with 5–10 ml of a physiological salt solution (PSS; the composition is given below) to remove the culture medium and debris. The cells were then equilibrated with the PSS for 5–8 min before current recording.

Recordings of whole-cell membrane currents were made at room temperature (23–27°C), using standard patch-clamp techniques (Hamill et al., 1981). Patch pipettes had a resistance of 3–5 MΩ when filled with a pipette solution. Command voltage pulses were generated by an electrical stimulator (SET-1201, Nihon Kohden, Shinjuku-ku, Tokyo), and the resulting current signals were amplified by a patch-clamp amplifier (CEZ-2300, Nihon Kohden) and stored on a pulse code modulation data recorder (RD-111T, TEAC, Musashino City, Tokyo) for analysis and illustration. Data analysis was performed on a computer (Macintosh Performa 5320, Apple, Cupertino, CA, USA), using a data acquisition and analysis instrument (MacLab4, ADInstruments, Castle Hill, NSW, Australia). The current signals were filtered at a cut-off frequency of 1 kHz and digitized with a sampling rate of 10–20 kHz.

NG108-15 cells express Na^+ currents and K^+ currents as well as I_{Ca} in response to depolarizing step pulses (Brown and Higashida, 1988). To detect I_{Ca} alone, the Na^+ current was blocked by tetrodotoxin (0.5 μM) added to the bathing solution, and the K^+ current was blocked by tetraethylammonium chloride (25 mM) added to the bathing solution and by dialysis with a CsCl-rich solution included in the patch pipettes (the composition is given below). The amplitude of I_{Ca} was estimated using a leak subtraction method as follows. In each experiment, a 10-mV hyperpolarizing pulse was applied at a holding potential of −80 mV, and the amplitude of the resulting current was regarded as a leakage current for each 10-mV step. The leakage current commensurate with the required step was then subtracted from the inward current evoked by the depolarizing step, assuming that the leakage did not rectify over the potential range studied. The capacitive component of the hyperpolarizing pulse-evoked current was integrated and calculated as the membrane capacitance of the cell.

The values in the text are expressed as means ± S.E.M. with the number of cells (n) used for measurements.

Statistical significance was tested using a Student's unpaired *t*-test and differences were considered significant when $P < 0.05$.

2.4. Solutions and drugs

PSS used in the experiments had the following composition (mM): NaCl 100, tetraethylammonium chloride 25, CsCl 5, $CaCl_2$ 2.5, $MgCl_2$ 1, glucose 25, 2-[4-(2-hydroxyethl)-1-piperazinyl]ethanesulfonic acid (HEPES) 5 (titrated to pH 7.4 with NaOH). The CsCl-rich pipette solution had the following composition (mM): CsCl 120, NaCl 10, $MgCl_2$ 2.5, NaGTP 0.1, glucose 5, HEPES 5, EGTA 0.05 (titrated to pH 7.2 with CsOH).

Tetrodotoxin, carbachol chloride, and ethylene glycol-bis (β-aminoethyl ether) *N,N,N′,N′*-tetraacetic acid (EGTA) were purchased from Wako (Osaka City, Osaka, Japan), and N^6, 2′-*O*-dibutyryladenosine 3′: 5′-cyclic monophosphate (dibutyryl cyclic AMP), 3-isobutyl-1-methylxanthine (IBMX), forskolin and noradrenaline were from Sigma (St. Louis, MO, USA).

2.5. Application of drugs

Carbachol, noradrenaline, dibutyryl cyclic AMP, IBMX or forskolin was extracellularly applied by replacing the PSS bathing cells with drug-containing PSS several times within some 10 s. EGTA was intracellularly applied by allowing it to diffuse from the patch pipette filled with EGTA-containing solution into the cell.

3. Results

3.1. Microscopic observation

Rabies virus-infected or uninfected NG108-15 cells prepared on a coverslip were bathed in PSS and examined

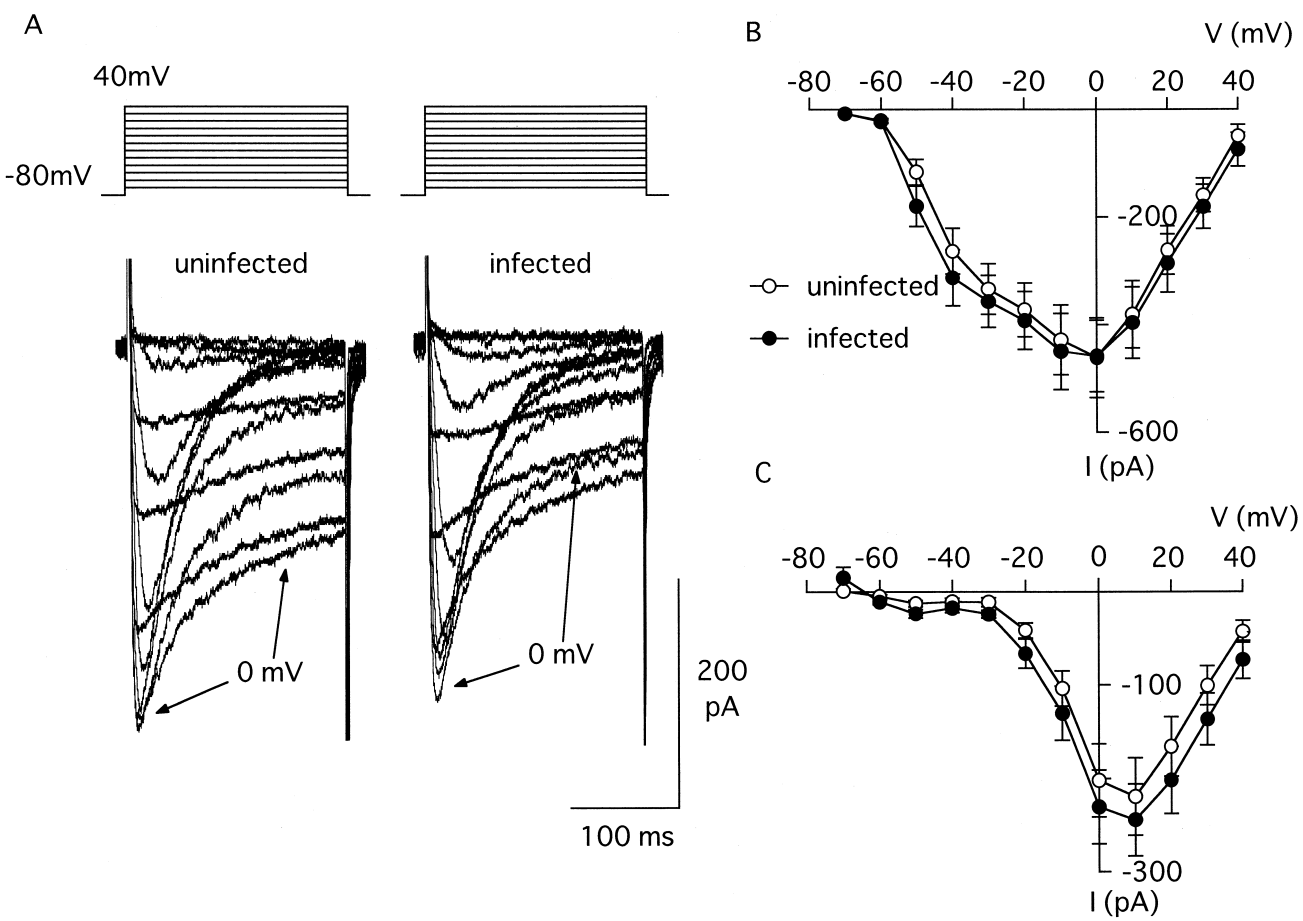

Fig. 1. Voltage-dependent Ca^{2+} current (I_{Ca}) in uninfected and infected NG108-15 cells. The cells were bathed in PSS to which tetrodotoxin (0.5 μM) and tetraethylammonium chloride (20 mM) were added, and held under voltage clamp at −80 mV using patch pipettes filled with a Cs-rich solution. Tetrodotoxin served to block Na^+ currents and both tetraethylammonium chloride and Cs^+ to block K^+ currents. To activate I_{Ca}, 200-ms step pulses to potentials ranging from −70 to 40 mV in 10-mV increments were applied every 10 s (upper traces in A). (A) Superimposed recording traces of I_{Ca} evoked by the sequential step pulses in an uninfected and an infected cell. (B) Averaged current–voltage relationships of peak I_{Ca} from 14 uninfected and 13 infected cells. (C) Averaged current–voltage relationships of late I_{Ca} measured at the end of step pulses from the same uninfected and infected cells as in (B). The symbols for both groups of cells in (B) are applicable in (C). Each point in (B) and (C) indicates the mean ± S.E.M. (vertical lines).

under a light microscope (×400). On day 2 after virus infection, there was no appreciable difference in morphological appearance between infected and uninfected cells, as previously described for mouse neuroblastoma cells (Iwata et al., 1999). Most of the cells (80–85%) had a round cell body of 30 to 40 μm in diameter with no visual neurites. The remaining cells had one or more neurites of 5 to 100 μm in length and a greater variation in cell size. Cells with a round shape of 30–40 μm in diameter and no neurites and which were separated from any neighboring cells were chosen for the following patch-clamp investigation.

When observed on day 3 after virus infection, cells seemed to be less able to attach themselves to the surface of a glass coverslips, so that perfusing the organ bath with PSS (Section 2.3 in Materials and methods) resulted in the loss of many cells. Such situations are considered to indicate some deterioration of cells (Ohashi and Komori, 1998). The remaining cells on the coverslip had smaller cell bodies than desired, and their cell membranes were less smooth than those of time-matched uninfected cells. In addition, it was difficult to establish the whole-cell patch-clamp configuration in these cells. For these reasons, cells infected with virus for longer than 2 days were not used for the present study.

3.2. Effect of rabies virus infection on ICa

I_{Ca} was recorded alternately from infected and uninfected cells under blockade of both Na^+ currents and K^+ currents (see Materials and methods). Cells were held at −80 mV and stepped every 10 s with 200-ms pulses to potentials ranging from −70 to 40 mV in 10-mV increments. Fig. 1A shows superimposed recording traces of I_{Ca} evoked by the sequential step pulses in an uninfected cell and in an infected cell. I_{Ca} reached a peak within 20 ms after the beginning of step pulses and then declined. As the stepped potential was increased, the amplitude of I_{Ca} increased over the negative range of the applied step potentials, but decreased over the positive range of the applied step potentials. Fig. 1B shows the averaged current–voltage relationship for peak I_{Ca} in 14 uninfected

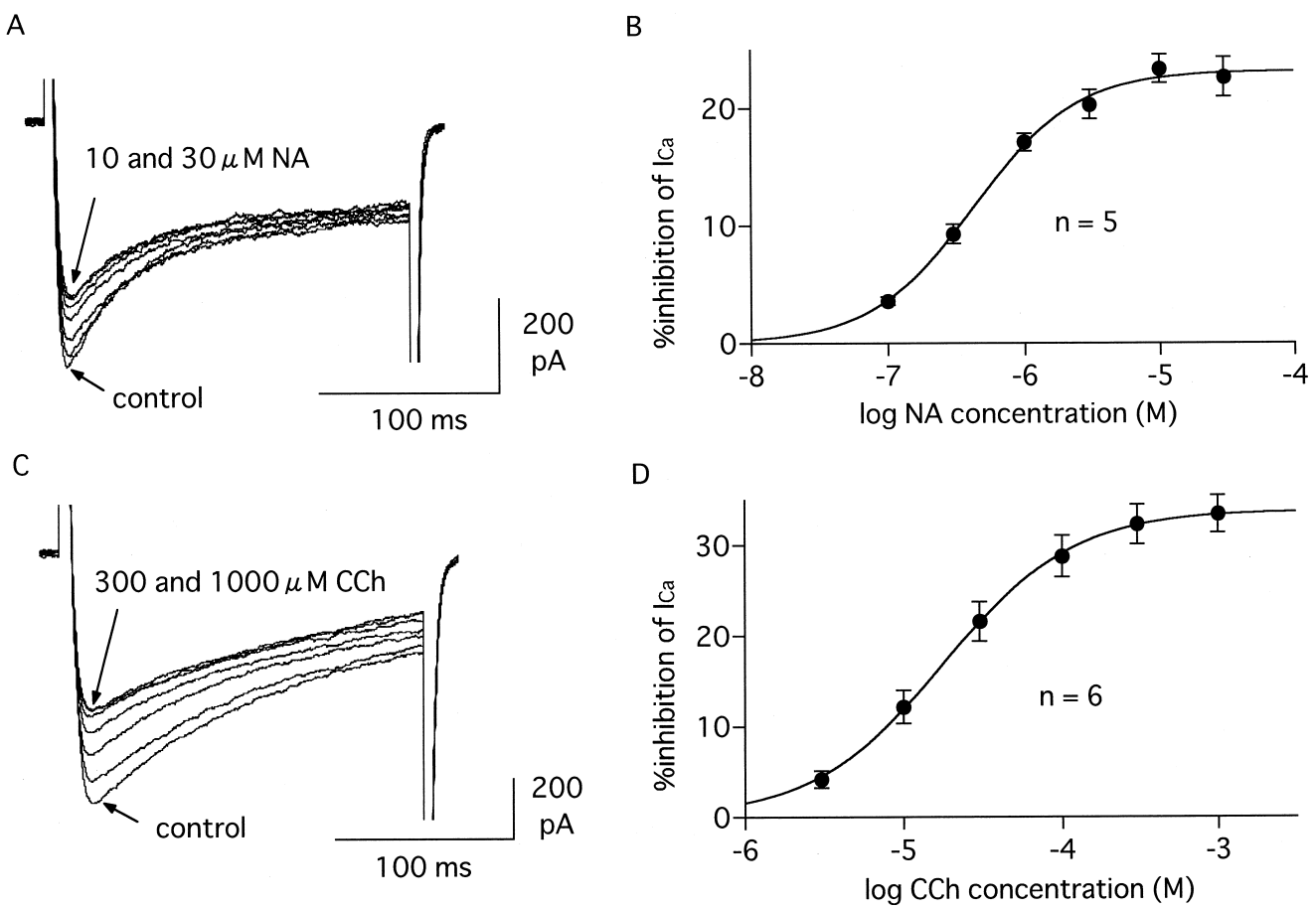

Fig. 2. Effects of noradrenaline (NA) and carbachol (CCh) on I_{Ca} in uninfected cells. I_{Ca} was repeatedly elicited every 10 s using a 200-ms step pulse from −80 to 0 mV, during which NA or CCh was applied in stepwise increasing concentrations (0.1, 0.3, 1, 3, 10, and 30 μM for NA and 3, 10, 30, 100, 300 and 1000 μM for CCh) within 3 min. (A) and (C) Superimposed recording traces of I_{Ca} before (control) and during the cumulative application of NA or CCh, respectively. Either agonist concentration dependently reduced I_{Ca}, in which the maximum inhibition was attained at 10 μM for NA and 300 μM for CCh. (B) and (D) Concentration–response curves for the NA- and CCh-induced I_{Ca} inhibition, respectively. The magnitude of I_{Ca} inhibition is expressed as a percentage of the control. Each point indicates the mean ± S.E.M. (vertical lines) of the number of measurements indicated.

cells and that in 13 infected cells, which almost overlap each other over the whole range of step potentials. The current–voltage relationships for the I_{Ca} remaining at the end of step pulses (late I_{Ca}) are shown in Fig. 1C. The late I_{Ca} was presumed not to contain a I_{Ca} component carried through the low-voltage-activated Ca^{2+} channels, because this type of Ca^{2+} channel is almost completely inactivated within 100 ms of its activation (Kasai and Neher, 1992). The current–voltage relationship for the late I_{Ca} was also not significantly different between infected and uninfected cells (Fig. 1C).

The time course of inactivation of I_{Ca} with a maximum amplitude, which was elicited by stepping to 0 mV, could be expressed by a two-phase exponential decay equation, $y = S_1 \cdot \exp(-t/\tau_1) + S_2 \exp(-t/\tau_2)$, where y is the current amplitude, t is time from the start of the step pulse, S_1 and S_2 are apparent amplitudes at $t = 0$ of the fast and slow inactivating current components, respectively, and τ_1 and τ_2 are decay time constants for the two components. In infected cells, mean values for S_1, τ_1, S_2 and τ_2 were 236 ± 29 pA, 33 ± 2 ms, 302 ± 60 pA and 1098 ± 219 ms ($n = 13$), respectively. Each of these mean values was not significantly different from the corresponding value in uninfected cells (S_1, 258 ± 42 pA; τ_1, 41 ± 5 ms; S_2, 279 ± 51 pA; τ_2, 903 ± 301 ms; $n = 14$).

Membrane capacitance was estimated from the capacitive current evoked by a 10-mV hyperpolarizing pulse (see Materials and methods). The mean value of 47.3 ± 5.3 pF ($n = 13$) in infected cells was not significantly different from that of 51.0 ± 3.7 pF ($n = 14$) in uninfected cells.

These results showed that rabies virus infection had no effect on the functional expression of voltage-dependent Ca^{2+} channels.

3.3. Effect of rabies virus infection on agonist-induced inhibition of ICa

In NG108-15 cells, activation of α_2-adrenoceptors with noradrenaline or muscarinic receptors with carbachol has been shown to reduce I_{Ca} (Docherty and McFadzean, 1989; Caulfield and Brown, 1991). In fact, when nor-

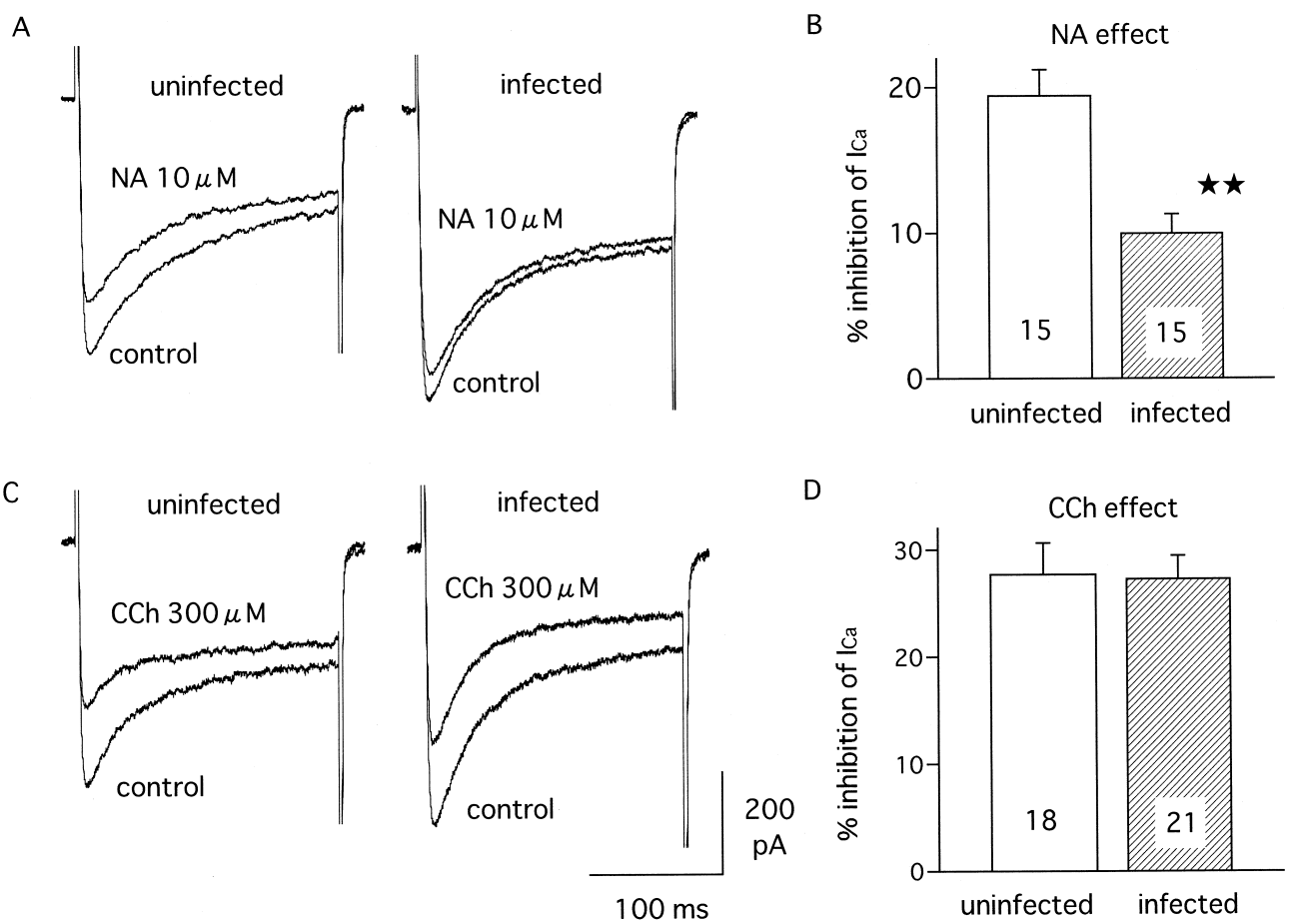

Fig. 3. Effect of rabies virus infection on NA- and CCh-induced I_{Ca} inhibition. The cells were held at −80 mV and I_{Ca} was elicited by 200-ms step pulses to 0 mV. (A) and (C) Superimposed recording traces of I_{Ca} before (control) and after application of NA (10 μM) in an uninfected and an infected cell, and the corresponding traces before (control) and after application of CCh (300 μM) in another uninfected and infected cell, respectively. (B) and (D) Comparison of I_{Ca} inhibition by NA between uninfected and infected cells and similar comparison of I_{Ca} inhibition by CCh, respectively. Each column indicates the mean with one S.E.M. (vertical lines) of the number of measurements indicated in the column. Note that the I_{Ca}-reducing effect of NA in infected cells significantly (★★$P < 0.01$) differed from that in uninfected cells.

adrenaline (0.1–30 μM) or carbachol (3–1000 μM) was applied in stepwise increasing concentrations to uninfected cells in which I_{Ca} was elicited every 10 s with a 200-ms step pulse to 0 mV, both drugs reduced peak I_{Ca} in a concentration-dependent manner. With noradrenaline, 10 and 0.4 μM were required to produce the maximum effect and half-maximum effect (IC_{50}), respectively (Fig. 2A and B). The maximum percent inhibition of I_{Ca} produced at 10 μM was 23.4 ± 1.2% ($n = 5$). With carbachol, the maximum effect was attained at 300 μM and IC_{50} was estimated to be 17.8 μM (Fig. 2C and D). The maximum percent inhibition of I_{Ca} produced at 300 μM was 32.3 ± 2.2% ($n = 6$), which was significantly greater ($P < 0.05$) than the corresponding value for 10 μM noradrenaline. The inhibitory effects of noradrenaline and carbachol were reversible, and they were blocked by yohimbine, an α_2-adrenoceptor antagonist (30 μM), and atropine, a muscarinic receptor antagonist (1 μM), respectively (data not shown). In the following experiments, unless otherwise stated, 10 μM noradrenaline and 300 μM carbachol were used to inhibit I_{Ca} evoked by stepping to 0 mV for 200 ms.

The inhibitory effect of noradrenaline on I_{Ca} was tested alternately in infected and uninfected cells (Fig. 3A). The percent inhibition of I_{Ca} varied from 4% to 16% among different infected cells, giving a mean value of 9.9 ± 1.3% ($n = 15$). This value was significantly smaller ($P < 0.01$) than the corresponding value of 19.4 ± 1.8% (8% to 33%, $n = 15$) in uninfected cells (Fig. 3B). When noradrenaline was applied at 100 μM instead of 10 μM to infected cells, I_{Ca} was decreased only by 7.0 ± 1.4% ($n = 11$). In uninfected cells, it was decreased by 16.2 ± 1.5% ($n = 13$).

In contrast, the inhibitory effect of carbachol on I_{Ca} remained almost unchanged after the viral infection. The percent inhibition of I_{Ca} was 27.3 ± 2.1% ($n = 21$) in infected cells and 27.7 ± 2.9% ($n = 18$) in uninfected cells (Fig. 3C and D).

These results showed that rabies virus infection attenuates α_2-adrenoceptor-mediated I_{Ca} inhibition without changing muscarinic receptor-mediated I_{Ca} inhibition.

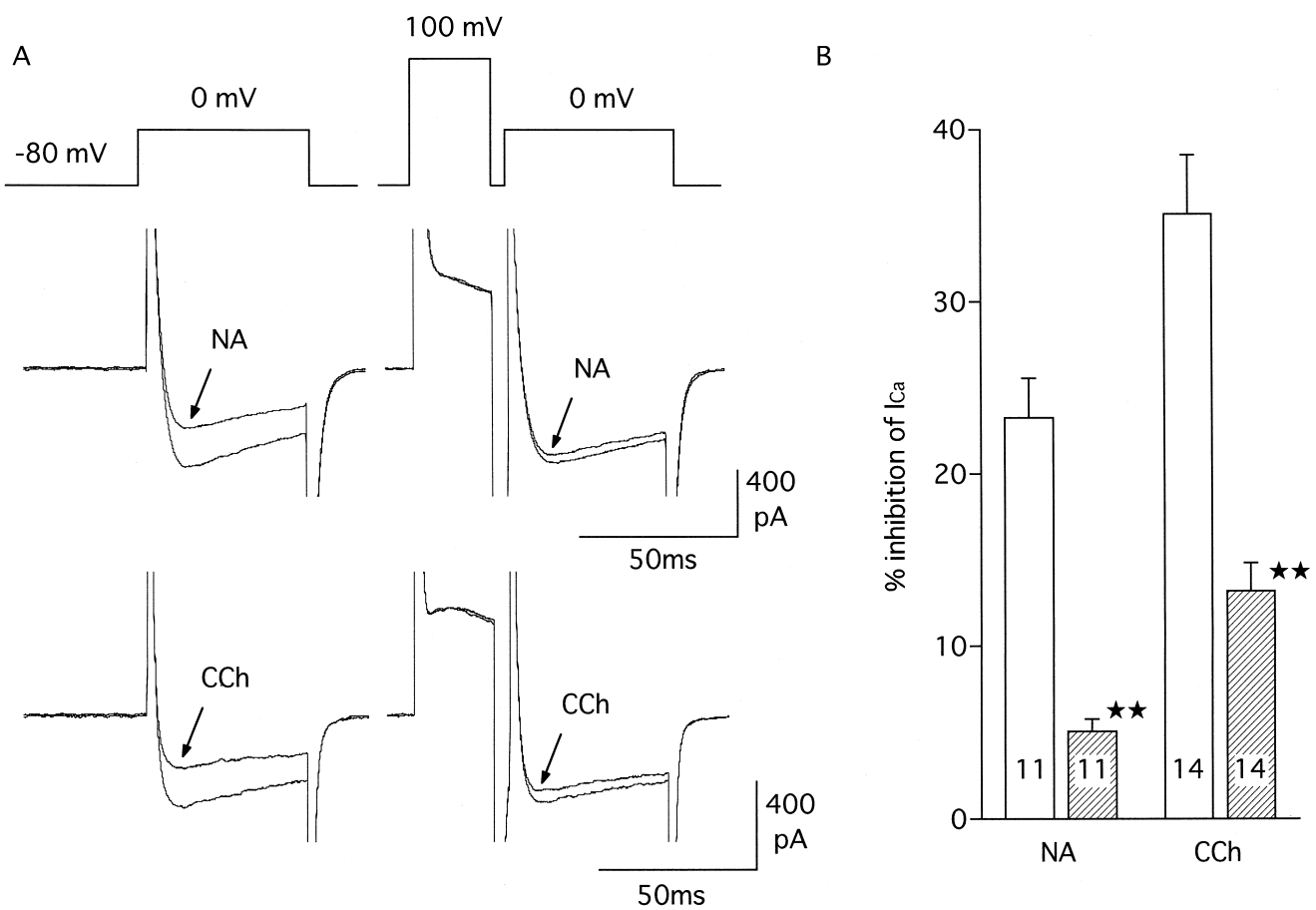

Fig. 4. Effect of pre-displacement of the membrane potential on NA- and CCh-induced I_{Ca} inhibition in uninfected cells. The cells were held at −80 mV, and I_{Ca} was elicited every 10 s using a 50-ms test pulse to 0 mV that was alternately preceded and not preceded by a 25-ms conditioning pulse to 100 mV (see top traces in A). (A) Superimposed recording traces of I_{Ca} elicited by the test pulses alone and with the conditioning pulse before and after application of 10-μM NA (middle traces) in a cell and before and after application of 300-μM CCh in another cell (bottom traces). (B) Summarized percent inhibition of I_{Ca} by NA and CCh, in which open and hatched columns indicate the data for I_{Ca} elicited by the test pulses without and with the conditioning pulse, respectively. Each column shows the mean with one S.E.M. (vertical lines) for the number of cells indicated. ★★, Significantly ($P < 0.01$) different from the value for I_{Ca} elicited by the test pulse alone.

3.4. Characterization of noradrenaline- and carbachol-induced ICa inhibition

To gain insight into the mechanism by which the noradrenaline-mediated inhibition of I_{Ca} was decreased after viral infection, the effects of noradrenaline and carbachol on I_{Ca} were compared in uninfected cells.

In cells treated with 20 mM EGTA to strongly buffer cytosolic Ca^{2+}, noradrenaline reduced I_{Ca} by $21.2 \pm 3.7\%$ ($n = 6$) and carbachol reduced I_{Ca} by $28.2 \pm 4.6\%$ ($n = 6$). The two mean values did not significantly differ from the respective control values ($19.4 \pm 1.8\%$ for noradrenaline and $27.7 \pm 2.9\%$ for carbachol; see above). In cells treated with forskolin (10 μM), an adenylate cyclase activator, and IBMX (100 μM), a phosphodiesterase inhibitor, the percent inhibition of I_{Ca} of $17.2 \pm 4.3\%$ ($n = 3$) for noradrenaline and $25.2 \pm 3.8\%$ ($n = 4$) for carbachol was not significantly different from the corresponding control values.

The agonist-induced I_{Ca} inhibition involving a direct interaction of G proteins with Ca^{2+} channels has been described to be relieved by briefly stepping to 100 mV or so (Swandulla et al., 1991). To test this, a 25-ms conditioning pulse to 100 mV was applied before stepping to a test potential of 0 mV to evoke I_{Ca}. The effect of noradrenaline or carbachol on the I_{Ca} was compared to that on I_{Ca} elicited by the test pulse without the conditioning pulse (see Fig. 4A and B). For noradrenaline, the percent inhibition of the former I_{Ca} was $5.1 \pm 0.7\%$ ($n = 11$), a value significantly smaller ($P < 0.01$) than the corresponding value ($23.3 \pm 2.3\%$) of the latter I_{Ca} (Fig. 4B). Substantially similar results were obtained with carbachol. The percent inhibition of I_{Ca} elicited by the test pulses with and without the conditioning pulse was $13.2 \pm 1.6\%$ and $35.1 \pm 3.4\%$ ($n = 14$), respectively (Fig. 4A and B).

Low-voltage-activated I_{Ca} was recorded separately from high-voltage-activated I_{Ca} using a two-pulse protocol such that two 80-ms step pulses to −30 and 20 mV were

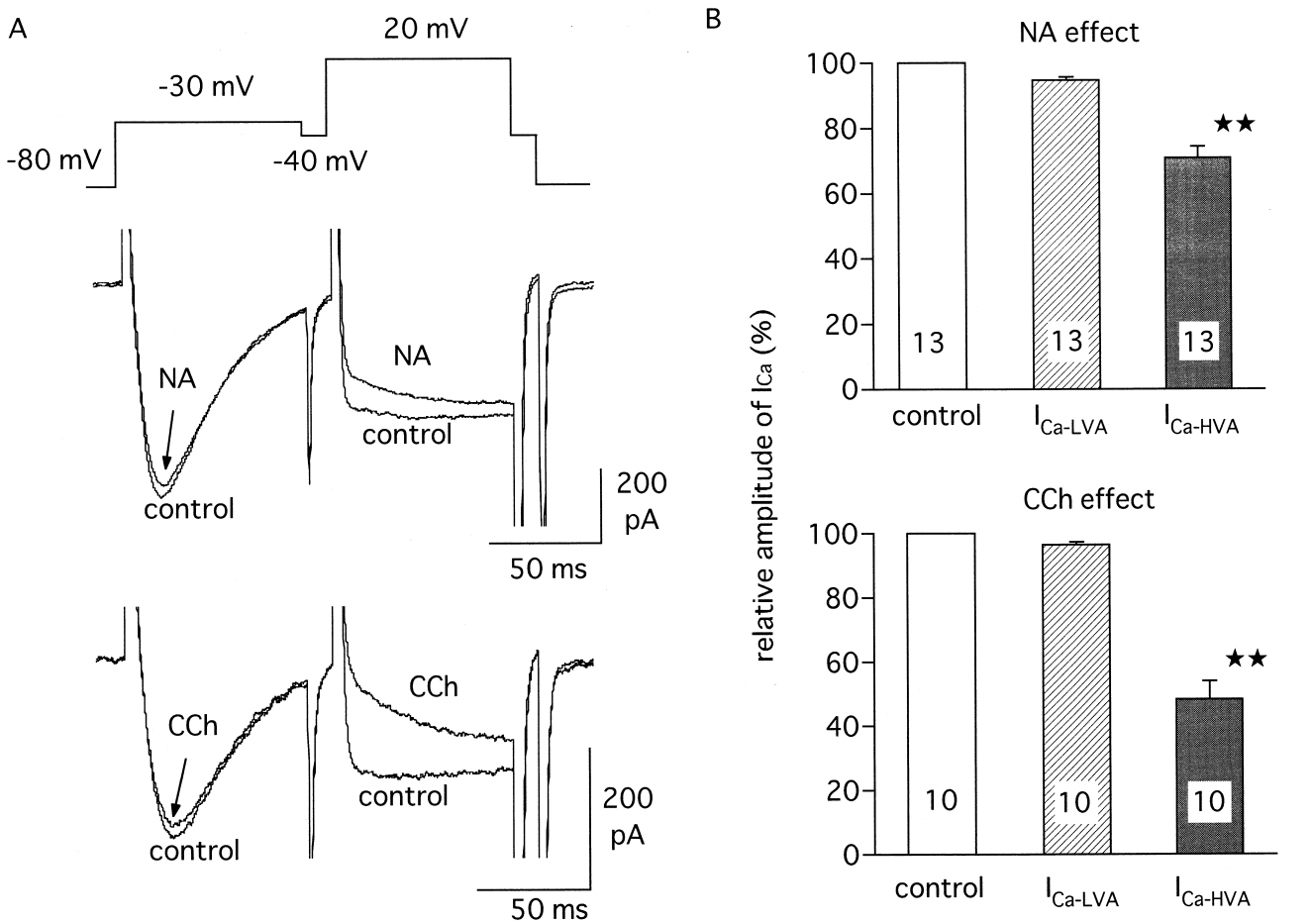

Fig. 5. Determination of I_{Ca} components inhibitable by NA and CCh in uninfected cells. A low-voltage-activated I_{Ca} and a high-voltage-activated I_{Ca} were successively evoked by a two-pulse protocol consisting of a pulse to −30 mV followed by another to 20 mV, as described by Kasai and Neher (1992) (see top trace in A). (A) Superimposed recording traces of I_{Ca} before (control) and after application of 10-μM NA in a cell (middle trace) and those before (control) and after application of 300-μM CCh in another cell (bottom trace). (B) Relative amplitudes of the low-voltage-activated I_{Ca} ($I_{Ca\text{-}LVA}$) and high-voltage-activated I_{Ca} ($I_{Ca\text{-}HVA}$) expressed as percentages of the respective controls, after application of NA (upper graph) and CCh (lower graph). The low-voltage-activated I_{Ca} was measured at its peak and the high-voltage-activated I_{Ca} at 10 ms after the beginning of the step pulse to 20 mV. Each column shows the mean with one S.E.M. (vertical lines) of measurements for the number of cells indicated. ★★, Significantly ($P < 0.01$) different from the control.

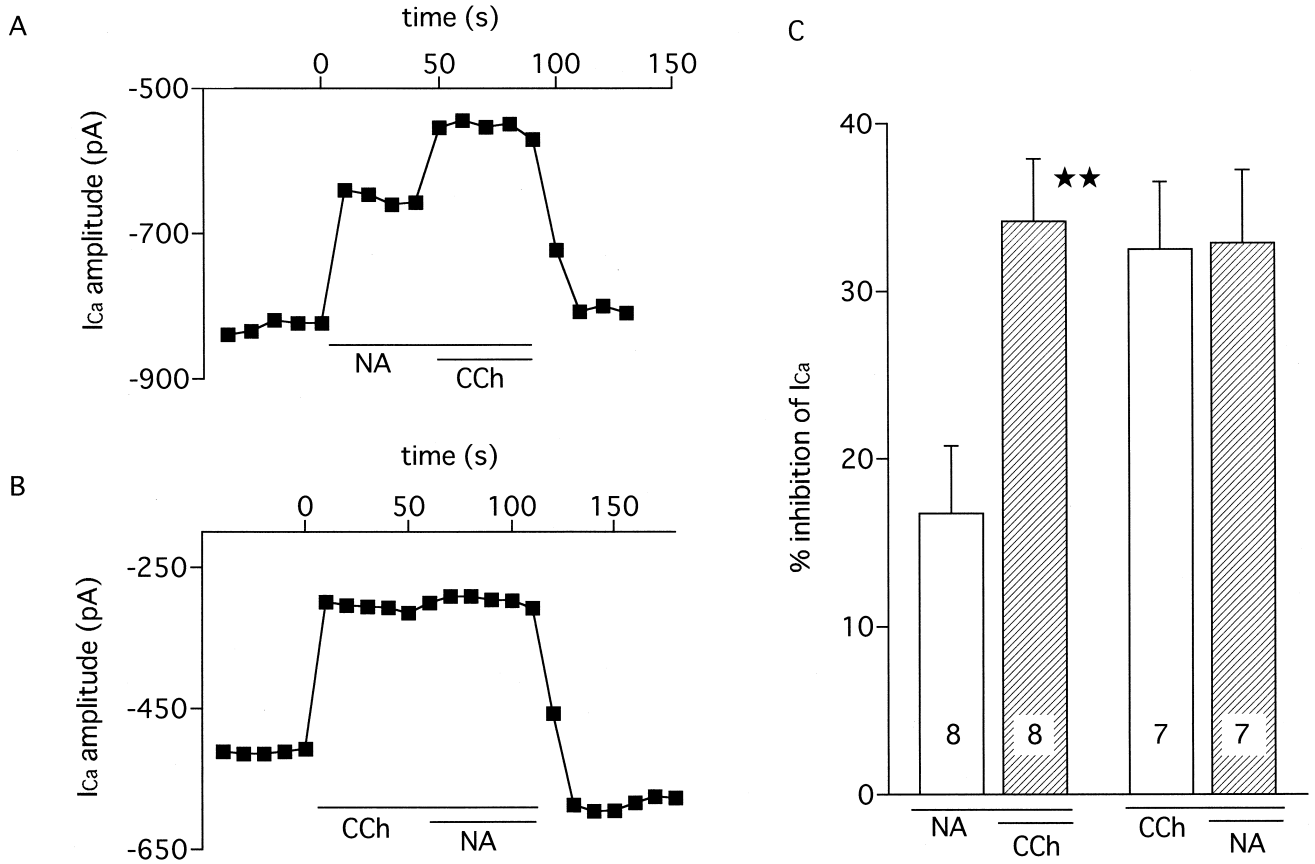

Fig. 6. Effects of a combination of NA and CCh on I_{Ca} in uninfected cells. The cells were held at −80 mV and I_{Ca} was elicited every 10 s using a 200-ms step pulse to 0 mV, during which either 10-μM NA or 300-μM CCh was first applied and then the other drug was applied in the presence of the first agonist. (A) The time course of the change in I_{Ca} amplitude during the application of NA followed by additional application of CCh. (B) The corresponding time course during application of CCh followed by additional application of NA. In (A) and (B), the start of the first agonist application is taken as time zero. (C) Summarized percent inhibition of I_{Ca} by the initial application of NA or CCh alone (open column) and by the subsequent application of both agonists (hatched column). Each column shows the mean with one S.E.M. (vertical lines) of measurements for the number of cells indicated. Note that CCh further significantly (★★, $P < 0.01$) reduced I_{Ca} in the presence of NA, but not vice versa.

applied successively with an interpulse interval of 10 ms, as described by Kasai and Neher (1992) (see Fig. 5A). The low-voltage-activated I_{Ca} was substantially unaffected by noradrenaline and carbachol (Fig. 5A and B), but the high-voltage-activated I_{Ca} was slowed in development and decreased in amplitude (Fig. 5A). The amplitude of the high-voltage-activated I_{Ca} measured at 10 ms after the start of the second step pulse was decreased to 70.8 ± 3.6% ($n = 13$) by noradrenaline and to 48.3 ± 5.6% ($n = 10$) by carbachol (Fig. 5B). Both agonists seemed likely to extensively suppress the high-voltage-activated Ca^{2+} channel.

Carbachol, when applied during the continued reduction of I_{Ca} by noradrenaline, was still effective in decreasing I_{Ca}. The percent inhibition of I_{Ca} by noradrenaline of 16.7 ± 4.0% was increased to 34.1 ± 3.8% ($n = 8$) after the additional application of carbachol (Fig. 6A and C). This was also seen even when a higher concentration (100 μM) of noradrenaline was used ($n = 2$). However, when carbachol was applied first, the subsequent application of noradrenaline produced no further reduction of I_{Ca}. The percent inhibition of I_{Ca} by carbachol alone was 32.5 ± 4.0% ($n = 7$) and that elicited by the additional application of noradrenaline was 32.9 ± 4.4% ($n = 7$) (Fig. 6B and C).

These characteristics of the inhibition of I_{Ca} produced by noradrenaline and carbachol did not indicate any difference in the mechanism of the action between these two agonists, although noradrenaline had a lower ceiling activity than carbachol.

4. Discussion

NG108-15 cells have been shown to express I_{Ca} carried through low-voltage-activated and high-voltage-activated Ca^{2+} channels upon step depolarization (Tsunoo et al., 1986). The low-voltage-activated I_{Ca} is characterized by a low-voltage threshold of some −50 mV for activation and a fast inactivation with a time constant of a few tens of milliseconds, and the high-voltage-activated I_{Ca} by a less negative voltage threshold of −30 to −20 mV for activation and a slower inactivation with a time constant of a few seconds (Docherty, 1988; Kasai and Neher, 1992). In

the present study, I_{Ca} was elicited by 200-ms step pulses to various potentials, so that peak I_{Ca} is thought to consist of the two types of I_{Ca}, of which the relative contributions vary depending on different step potentials. However, I_{Ca} measured at the end of step depolarizations (late I_{Ca}) does not contain the low-voltage-activated I_{Ca}, because this type of I_{Ca} has been completely inactivated during the early stepping period. There was no significant difference in the current–voltage relationships for peak I_{Ca} and late I_{Ca} between uninfected and infected cells. The inactivation phase of I_{Ca} could be described by a double exponential function in which fast and slow decay time constants of the two components were comparable with those reported for the low-voltage-activated I_{Ca} and for the high-voltage-activated I_{Ca}, respectively (Docherty, 1988), and apparent initial amplitudes remained unchanged after the viral infection. These findings suggest that the viral infection does not lead to any change in the functional expression of the two types of voltage-dependent Ca^{2+} channel.

It is of interest that rabies virus infection can differently modify the functional expression of different ion channels in the plasma membrane: voltage-dependent Na^+ channels and inward rectifier K^+ channels are sensitive to rabies virus infection (Iwata et al., 1999), but delayed rectifier K^+ channels and low-voltage-activated and high-voltage-activated Ca^{2+} channels are insensitive. This could possibly indicate that the virus infection causes selective functional impairment of the plasma membrane and that it does not act through a common mechanism that determines ion channel expression.

The viral infection attenuated the ability of α_2-adrenoceptors to inhibit I_{Ca} with no change in the ability of muscarinic receptors to inhibit I_{Ca}. Noradrenaline and carbachol were shown to act through a common mechanism independent of cytosolic Ca^{2+} and cyclic AMP, which suppresses the high-voltage-activated Ca^{2+} channel. These effects have previously been shown to be mediated by pertussis toxin-sensitive G proteins (McFadzean and Docherty, 1989; Higashida et al., 1990). The finding of relief of noradrenaline- and carbachol-induced $I(_{Ca})$ inhibition during membrane depolarization to 100 mV (see Fig. 4) suggests the involvement of a direct interaction of G proteins with Ca^{2+} channels, as described for γ-aminobutyric acid-induced I_{Ca} inhibition in chick sensory neurons (Swandulla et al., 1991). The question of how the viral infection can solely attenuate α_2-adrenoceptor-mediated I_{Ca} inhibition remains to be answered. However, it is possible that the site of action of the viral infection may be located at the level of receptors rather than the downstream signaling pathway. A possible explanation for the action of the viral infection is inhibition of synthesis and/or intracellular transport of α_2-adrenoceptor proteins and a decrease in the distribution of the receptor in the plasma membrane. Radioligand binding studies have previously suggested reduced specific binding sites for neurotransmitters such as acetylcholine and serotonin in the cell membrane (Tsiang, 1982; Ceccaldi et al., 1993). Another possibility is that rabies virus infection impairs the function of α_2-adrenoceptors to activate G proteins responsible for I_{Ca} inhibition. In NG108-15 cells, G protein coupling of opiate receptors has been demonstrated to be disrupted after infection with rabies virus (Koschel and Munzel, 1984). Recent mutagenesis studies of G protein-coupled receptors including α_2-adrenoceptors have shown that a point mutation of these receptors blocks interaction with G proteins (Wess, 1993; Surprenant et al., 1992). Further study is needed to identify the changes at the receptor level caused by the viral infection, which result in the attenuation of α_2-adrenoceptor-mediated I_{Ca} inhibition.

The viral infection for 2 days hardly had any effect on the muscarinic inhibition of I_{Ca}. However, this does not necessarily exclude the possibility that a longer infection, if the cells survive, causes modulation of the muscarinic effect. To test this, it will be necessary to carry out further infection experiments with lower infection multiplicities than used in the present study (50 plaque forming units per cell).

In the central nervous system, α_2-adrenoceptor-mediated inhibition of I_{Ca} is believed to serve as a brake mechanism to keep neurons such as noradrenergic neurons from releasing their transmitters beyond physiological requirements (Starke et al., 1989). Administration of α_2-adrenoceptor antagonists induces increased aggressive or anxious behavior in rats and monkeys, and accelerates lidocaine-induced convulsions in mice, possibly through excessive release of catecholamines (Haller et al., 1994; Rosenblum et al., 1991; Altenburg and Farah, 1999). Thus, the present finding of the reduced function of α_2-adrenoceptors in inhibiting I_{Ca} may provide some insight into the pathogenesis of rabies disease, which is accompanied by hyperexcited symptoms such as aggressive behavior and general convulsions (Hemachudha and Phuapradit, 1997).

In conclusion, in NG108-15 cells, rabies virus infection causes no noticeable change in the functional expression of voltage-dependent Ca^{2+} channels, but it attenuates the α_2-adrenoceptor-mediated inhibition of Ca^{2+} channel activity. The inhibitory effect may arise from some change at the receptor level but not in the downstream signaling pathway.

Acknowledgements

This work was supported by a grant-in-aid for scientific research (10306020) from the Ministry of Education, Science and Culture, Japan.

References

Altenburg, S.P., Farah, M.B., 1999. Tizanidine protects mice against convulsions induced by lidocaine: involvement of α_2-adrenoceptors. Pharmacol. Toxicol. 84, 29–33.

Brown, D.A., Higashida, H., 1988. Voltage- and calcium-activated potassium currents in mouse neuroblastoma×rat glioma hybrid cells. J. Physiol. 397, 149–165.

Caulfield, M.P., Brown, D.A., 1991. Pharmacology of the putative M_4 muscarinic receptor mediating Ca-current inhibition in neuroblastoma ×glioma hybrid (NG 108-15) cells. Br. J. Pharmacol. 104, 39–44.

Ceccaldi, P.E., Fillion, M.P., Ermine, A., Tsiang, H., Fillion, G., 1993. Rabies virus selectively alters 5-HT_1 receptor subtypes in rat brain. Eur. J. Pharmacol. 245, 129–138.

Docherty, R.J., 1988. Gadolinium selectively blocks a component of calcium current in rodent neuroblastoma×glioma hybrid (NG108-15) cells. J. Physiol. 398, 33–47.

Docherty, R.J., McFadzean, I., 1989. Noradrenaline-induced inhibition of voltage-sensitive calcium currents in NG 108-15 hybrid cells. Eur. J. Neurosci. 1, 132–140.

Dumrongphol, H., Srikiatkhachorn, A., Hemachudh, T., Kotchabhakdi, N., Govitrapong, P., 1996. Alteration of muscarinic acetylcholine receptors in rabies viral-infected dog brains. J. Neurol. Sci. 137, 1–6.

Haller, J., Barna, I., Kovacs, J.L., 1994. α_2-Adrenoceptor blockade, pituitary–adrenal hormones, and agonistic interactions in rats. Psychopharmacology (Berlin) 115, 478–484.

Hamill, O.P., Marty, A., Neher, E., Sakmann, B., Sigworth, F.J., 1981. Improved patch-clamp techniques for high-resolution current recording from cells and cell-free membrane patches. Pfluegers Arch. 391, 85–100.

Hemachudha, T., Phuapradit, P., 1997. Rabies. Curr. Opin. Neurol. 10, 260–267.

Higashida, H., Hashii, M., Fukuda, K., Caulfield, M.P., Numa, S., Brown, D.A., 1990. Selective coupling of different muscarinic acetylcholine receptors to neuronal calcium currents in DNA-transfected cells. Proc. R. Soc. London B: Biol. Sci. 242, 68–74.

Ito, H., Minamoto, N., Watanabe, T., Goto, H., Rong, L.T., Sugiyama, M., Kinjo, T., Mannen, K., Mifune, K., Konobe, T., Yoshida, I., Takamizawa, A., 1994. A unique mutation of glycoprotein gene of the attenuated RC-HL strain of rabies virus, a seed virus used for production of animal vaccine in Japan. Microbiol. Immunol. 38, 479–482.

Iwata, M., Komori, S., Unno, T., Minamoto, N., Ohashi, H., 1999. Modification of membrane currents in mouse neuroblastoma cells following infection with rabies virus. Br. J. Pharmacol. 126, 1691–1698.

Johnson, R.T., 1965. Experimental rabies. Studies of cellular vulnerability and pathogenesis using fluorescent antibody staining. J. Neuropathol. Exp. Neurol. 24, 662–674.

Kasai, H., Neher, E., 1992. Dihydropyridine-sensitive and ω-conotoxin-sensitive calcium channels in a mammalian neuroblastoma–glioma cell line. J. Physiol. 448, 161–188.

Koschel, K., Munzel, P., 1984. Inhibition of opiate receptor-mediated signal transmission by rabies virus in persistently infected NG-108-15 mouse neuroblastoma–rat glioma hybrid cells. Proc. Natl. Acad. Sci. U. S. A. 81, 950–954.

McFadzean, I., Docherty, R.J., 1989. Noradrenaline- and enkephalin-induced inhibition of voltage-sensitive calcium currents in NG108-15 hybrid cells. Eur. J. Neurosci. 1, 141–147.

Minamoto, N., Tanaka, H., Hishida, M., Goto, H., Ito, H., Naruse, S., Yamamoto, K., Sugiyama, M., Kinjo, T., Mannen, K., Mifune, K., 1994. Linear and conformation-dependent antigenic sites on the nucleoprotein of rabies virus. Microbiol. Immunol. 38, 449–455.

Munzel, P., Koschel, K., 1981. Rabies virus decreases agonist binding to opiate receptors of mouse neuroblastoma–rat glioma hybrid cells 108-CC-15. Biochem. Biophys. Res. Commun. 101, 1241–1250.

Murphy, F.A., 1977. Rabies pathogenesis. Arch. Virol. 54, 279–297.

Ohashi, H., Komori, S., 1998. Isolation of intestinal smooth muscle cells. In: Preedy, V.R., Watson, R.R. (Eds.), Methods in Disease: Investigating the Gastrointestinal Tract. Greenwich Medical Media, London, pp. 253–260.

Rosenblum, L.A., Coplan, J.D., Friedman, S., Bassoff, T., 1991. Dose–response effects of oral yohimbine in unrestrained primates. Biol. Psychiatry 29, 647–657.

Starke, K., Göthert, M., Kilbinger, H., 1989. Modulation of neurotransmitter release by presynaptic autoreceptors. Physiol. Rev. 69, 864–989.

Surprenant, A., Horstman, D.A., Akbarali, H., Limbird, L.E., 1992. A point mutation of the α_2-adrenoceptor that blocks coupling to potassium but not calcium currents. Science 257, 977–980.

Swandulla, D., Carbone, E., Lux, H.D., 1991. Do calcium channel classifications account for neuronal calcium channel diversity?. Trends Neurosci. 14, 46–51.

Tirawatnpong, S., Hemachudha, T., Manutsathit, S., Shuangshoti, S., Phanthumchinda, K., Phanuphak, P., 1989. Regional distribution of rabies viral antigen in central nervous system of human encephalitic and paralytic rabies. J. Neurol. Sci. 92, 91–99.

Tsiang, H., 1982. Neuronal function impairment in rabies-infected rat brain. J. Gen. Virol. 61, 277–281.

Tsunoo, A., Yoshii, M., Narahashi, T., 1986. Block of calcium channels by enkephalin and somatostatin in neuroblastoma–glioma hybrid NG108-15 cells. Proc. Natl. Acad. Sci. U. S. A. 83, 9832–9836.

Wess, J., 1993. Molecular basis of muscarinic acetylcholine receptor function. Trends Pharmacol. Sci. 14, 308–313.